Accuracy and conservation characteristics of the numerical algorithm in Environment Canada's ONE-D model

Faye Hicks

Abstract: Environment Canada's One-Dimensional Hydrodynamic Model is built upon Gunaratnam's six-point, implicit finite difference scheme which was developed at the Massachusetts Institute of Technology in 1970. Many of the details of the implementation of the numerical scheme, and its appropriate use, are available only in the original unpublished references. Therefore, it is appropriate to examine the numerical behavior of the implemented scheme in order to determine optimal relative time and space step increments and also to identify any potential limitations in the applicability of the model. This paper examines these issues through a Fourier analysis of the stability and accuracy characteristics of this numerical scheme. The validity of the results of this linear stability analysis are verified through nonlinear wave propagation tests. It is concluded that the current guidelines regarding the recommended relationship between the time and space step increments and the number of nodes used to describe a wave profile should be changed. Adequate results can be obtained at reasonable spatial discretizations by limiting the Courant number to 0.5 or less.

Key words: St. Venant, Fourier analysis, ONE-D, Environment Canada.

Résumé : Le modèle hydrodynamique unidimensionnel d'Environnement Canada est bâti sur l'arrangement implicite par éléments finis à six-points de Gunaratnam qui a été développé au Massachussetts Institute of Technology en 1970. Plusieurs des détails de mise en oeuvre de cet arrangement numérique et de son utilisation appropriée sont seulement disponibles dans les références originales non publiées. Ainsi, il est approprié d'examiner le comportement numérique du modèle mis en oeuvre afin de déterminer les pats d'augmentations relatives optimales de temps et d'espace, et aussi d'identifier toutes limitations potentielles dans l'applicabilité du modèle. Cet article examine ces problèmes à travers une analyse de Fourier de la stabilité et précision de cet arrangement numérique. La validité des résultats de cette analyse de stabilité linéaire est vérifiée à travers des essais de propagation non-linéaire d'ondes. Il est conclu que les directives courantes relatives à la relation recommandée entre les pats d'augmentation de temps et d'espace et le nombre de noeuds utilisés pour décrire un profil d'onde doivent être changées. Des résultats adéquats peuvent être obtenus avec une discrétisation spatiale raisonnable en limitant le nombre Courant à 0,5 ou moins.

Mots clés : St-Venant, analyse de Fourier, ONE-D, Environnement Canada.
[Traduit par la Rédaction]

Introduction

The One-Dimensional Hydrodynamic Model (ONE-D) is an unsteady flow model which was developed by Environment Canada for the analysis of wave propagation problems in open channels. The model is extensively used by Environment Canada specialists in the analysis of a variety of complex open channel flow problems in rivers and tidal estuaries, and has been adapted to handle simple ice covers, sediment transport, and channel networks. It is currently being incorporated into Environment Canada's river ice model, RIVICE (Martinson et al. 1993).

Received July 5, 1996.
Revised manuscript accepted December 16, 1996.

F. Hicks. Department of Civil Engineering, University of Alberta, Edmonton, AB T6G 2G7, Canada.

Written discussion of this article is welcomed and will be received by the Editor until December 31, 1997 (address inside front cover).

The ONE-D model employs a numerical scheme which was developed at the Massachusetts Institute of Technology (MIT) more than 25 years ago (Gunaratnam and Perkins 1970). Many of the details of the ONE-D implementation, and of the known behavior of the underlying numerical scheme, are available only in the original MIT reports (Gunaratnam and Perkins 1970; Daily and Harleman 1972; Wood et al. 1972), which are not easily obtained. Given the extensive use of the ONE-D model in Canada today, it is of value to examine the numerical behavior of the implemented scheme to determine optimal discretizations and to identify potential limitations in the applicability of the model.

This paper provides a review of the available information regarding the numerical scheme implemented in the ONE-D model, as well as details of the symmetric formulation used. Then, a Fourier analysis is used to assess the stability and accuracy of the implemented numerical scheme. The validity of these results, and the conservation characteristics of the implemented scheme, are then examined through nonlinear wave propagation tests. The results of these analyses are used

to establish new guidelines for optimum time and space step relationships.

Equations modelled

The ONE-D model is a one-dimensional, unsteady, open channel flow model based on a formulation of the St. Venant equations which uses discharge, Q, and water surface elevation, z, as the dependent variables (Environment Canada 1988):

$$[1] \quad B\frac{\partial z}{\partial t} + \frac{\partial Q}{\partial x} = q_L$$

$$[2] \quad \frac{\partial Q}{\partial t} + 2V\frac{\partial Q}{\partial x} + gA(1 - \mathrm{Fr}^2)\frac{\partial z}{\partial x} = gA\left\{\frac{\mathrm{Fr}^2}{B}\frac{\partial A^z}{\partial x} - S_f\right\}$$

where x is the longitudinal coordinate; t is the temporal coordinate; B is the total top width of a cross section; z is the water surface elevation; Q is discharge; q_L is the lateral inflow; V is the cross-sectionally averaged longitudinal velocity; g is acceleration due to gravity; A is the cross-sectional area perpendicular to flow; Fr is the Froude number; and S_f is the friction slope; and

$$[3] \quad \frac{\partial A^z}{\partial x} = \left.\frac{\partial A}{\partial x}\right|_{z\,=\,\text{constant}}$$

which represents non-prismatic channel effects.

Although the equations do not explicitly appear in the program documentation, the ONE-D model is actually based on the following symmetric formulation of these equations (Environment Canada 1988; Dailey and Harleman 1972; Gunaratnam and Perkins 1970; and the program source code, 1987-10-15):

$$[4] \quad \left\{\frac{\partial z}{\partial t} + \lambda_+\frac{\partial z}{\partial x}\right\} - \frac{1}{B\lambda_-}\left\{\frac{\partial Q}{\partial t} + \lambda_+\frac{\partial Q}{\partial x}\right\} = -\frac{gA}{B\lambda_-}\left\{\frac{\mathrm{Fr}^2}{B}\frac{\partial A^z}{\partial x} - S_f\right\} + \frac{q_L}{B}$$

$$[5] \quad \left\{\frac{\partial z}{\partial t} + \lambda_-\frac{\partial z}{\partial x}\right\} - \frac{1}{B\lambda_+}\left\{\frac{\partial Q}{\partial t} + \lambda_-\frac{\partial Q}{\partial x}\right\} = -\frac{gA}{B\lambda_+}\left\{\frac{\mathrm{Fr}^2}{B}\frac{\partial A^z}{\partial x} - S_f\right\} + \frac{q_L}{B}$$

where

$$[6] \quad \lambda_+ = V + c$$

$$[7] \quad \lambda_- = V - c$$

and

$$[8] \quad c = \sqrt{g\frac{A}{B}}$$

Equations [4] and [5] can be derived from [1] and [2] through linear transformation or simply by multiplying [1] successively by λ_+ and λ_-, and then subtracting the resulting equations from [2]. The results are quite different in appearance from the classical symmetric equations used in the method of characteristics, but the equivalence can be seen if we consider the simplified case of a horizontal, frictionless, rectangular channel of constant width, with no lateral inflow. In this case, [4] and [5] reduce to

$$[9] \quad \left\{\frac{\partial h}{\partial t} + \lambda_+\frac{\partial h}{\partial x}\right\} - \frac{1}{B\lambda_-}\left\{\frac{\partial Q}{\partial t} + \lambda_+\frac{\partial Q}{\partial x}\right\} = 0$$

$$[10] \quad \left\{\frac{\partial h}{\partial t} + \lambda_-\frac{\partial h}{\partial x}\right\} - \frac{1}{B\lambda_+}\left\{\frac{\partial Q}{\partial t} + \lambda_-\frac{\partial Q}{\partial x}\right\} = 0$$

in which h is the flow depth in the rectangular section. Rearranging and substituting for λ_+ and λ_-, we obtain

$$[11] \quad \left\{\frac{\partial Q}{\partial t} - B(V-c)\frac{\partial h}{\partial t}\right\} + (V+c)\left\{\frac{\partial Q}{\partial x} - B(V-c)\frac{\partial h}{\partial x}\right\} = 0$$

$$[12] \quad \left\{\frac{\partial Q}{\partial t} - B(V+c)\frac{\partial h}{\partial t}\right\} + (V-c)\left\{\frac{\partial Q}{\partial x} - B(V+c)\frac{\partial h}{\partial x}\right\} = 0$$

Focusing on [11] as an example and employing the following equalities:

$$[13] \quad \frac{\partial Q}{\partial t} = \frac{\partial AV}{\partial t} = A\frac{\partial V}{\partial t} + V\frac{\partial A}{\partial t}$$

$$[14] \quad -B(V-c)\frac{\partial h}{\partial x} = -V\frac{\partial A}{\partial x} + c\frac{\partial A}{\partial x}$$

substitution into [11] gives

$$[15] \quad \left\{A\frac{\partial V}{\partial t} + c\frac{\partial A}{\partial t}\right\} + (V+c)\left\{A\frac{\partial V}{\partial x} + c\frac{\partial A}{\partial x}\right\} = 0$$

Dividing through by Bc^2/g, and using the following equalities:

$$[16] \quad c = \sqrt{gh}, \qquad \partial h = \frac{2c}{g}\partial c$$

equation [15] reduces to

$$[17] \quad \left\{\frac{\partial V}{\partial t} + 2\frac{\partial c}{\partial t}\right\} + (V+c)\left\{\frac{\partial V}{\partial x} + 2\frac{\partial c}{\partial x}\right\} = 0$$

Similarly, [12] reduces to

$$[18] \quad \left\{\frac{\partial V}{\partial t} - 2\frac{\partial c}{\partial t}\right\} + (V-c)\left\{\frac{\partial V}{\partial x} - 2\frac{\partial c}{\partial x}\right\} = 0$$

Equations [17] and [18] combine to give the familiar equations:

$$[19] \quad \frac{\partial}{\partial t}(V \pm 2c) + (V \pm c)\left\{\frac{\partial}{\partial x} + (V \pm 2c)\right\} = 0$$

Potential limitations of this symmetric formulation

In comparing the symmetric formulation in [4] and [5] to the nonsymmetric formulation presented by [1] and [2], Gunaratnam and Perkins (1970) considered the symmetric formulation to be "much more accurate for numerical solution by implicit finite difference schemes because the coefficients of the resulting sets of equations are of the same order of magnitude, hence roundoff error has less effect on the overall solution." Although there may be some merit in this argument, this reasoning neglects consideration of the conservation properties of the formulation. Hicks and Steffler (1995) have found that, for finite element schemes at least, symmetric formulations of the

St. Venant equations display inferior mass and momentum conservation characteristics, when compared to nonsymmetric formulations.

Numerical solution method

In Environment Canada's ONE-D model, the unsteady flow equations presented in [4] and [5] are solved using Gunaratnam's six-point, implicit finite difference scheme (Environment Canada 1988; Gunaratnam and Perkins 1970). The equations are first linearized to

$$[20]\quad \left\{\frac{\partial z}{\partial t}(V \pm c)\frac{\partial z}{\partial x}\right\} - \frac{1}{B_o(V \mp c)}\left\{\frac{\partial Q}{\partial t} + (V \pm c)\frac{\partial Q}{\partial x}\right\} - \psi = 0$$

where B_o is a constant top width, and

$$[21]\quad \psi = -\frac{gA}{B_o(V \mp c)}\left\{\mathrm{Fr}^2\frac{\partial A^z}{\partial x} - S_f\right\} + \frac{q_L}{B_o}$$

in which $(V \pm c)$, $(V \mp c)$, and ψ are all assumed constant.

Gunaratnam and Perkins (1970) solved these linearized equations using a finite element weighted residual method, employing the Galerkin technique and setting the test functions equal to the basis functions. A fully implicit formulation was used. They also employed a uniform spatial discretization in order to implement this finite element scheme as a finite difference method (Dailey and Harleman 1972). In fact, Gunaratnam's six-point implicit finite difference scheme is a fully implicit, finite difference implementation of the Galerkin weighted residual finite element method known as the Bubnov–Galerkin finite element scheme. This finite difference implementation results in two equations for each (interior) computational node, specifically (Gunaratnam and Perkins 1970):

$$\begin{aligned}[22]\quad &\left(\frac{1}{6} - \frac{\Delta t}{\Delta x}\frac{(V \pm c)}{2}\right)Z_{j-1}^{n+1} \\ &+ \frac{2}{3}Z_j^{n+1} + \left(\frac{1}{6} - \frac{\Delta t}{\Delta x}\frac{(V \pm c)}{2}\right)Z_{j+1}^{n+1} \\ &- \frac{1}{B_o(V \mp c)}\left\{\left(\frac{1}{6} - \frac{\Delta t}{\Delta x}\frac{(V \pm c)}{2}\right)Q_{j-1}^{n+1}\right. \\ &\left. + \frac{2}{3}Q_j^{n+1} + \left(\frac{1}{6} - \frac{\Delta t}{\Delta x}\frac{(V \pm c)}{2}\right)Q_{j+1}^{n+1}\right\} \\ &= \psi + \left(\frac{1}{6}Z_{j-1}^{n} + \frac{2}{3}Z_j^{n} + \frac{1}{6}Z_{j+1}^{n}\right) \\ &\quad - \frac{1}{B_o(V \mp c)}\left(\frac{1}{6}Q_{j-1}^{n} + \frac{2}{3}Q_j^{n} + \frac{1}{6}Q_{j+1}^{n}\right)\end{aligned}$$

where n and j are the temporal and spatial indices, respectively, and Δx and Δt are the space and time step increments, respectively.

Potential limitations of this numerical scheme

In open channel flow applications, semi-implicit formulations of the Bubnov–Galerkin finite element scheme has been shown to be useful for modeling relatively flat waves but have been found to perform poorly in the vicinity of steep gradients in the solution, such as are experienced in transitions between supercritical and subcritical flows (Katapodes 1984). Instabilities (spurious oscillations) result and the solution deteriorates rapidly. One way to avoid such oscillations is to refine the discretization (use more nodes to describe the wave profile). An alternate approach is to employ the fully implicit formulation, as Gunaratnam and Perkins (1970) did, as it can be shown that a fully implicit formulation always causes numerical attenuation, guaranteeing stability. However, as will be illustrated with the Fourier analysis, this use of a fully implicit formulation introduces nonselective artificial diffusion into the solution, damping physical wave components as well as numerically generated instabilities.

Gunaratnam's finite difference implementation of this scheme operates on the linearized form of the equations, which is equivalent to conducting the first iteration in a nonlinear iterative solution. Linearization can mean significant computational time savings, as each iteration requires the solution of the computational matrix. However, when variables are changing quickly, as is the case for transcritical flows (transitions between subcritical and supercritical flows) and shock propagation problems, the linearized solution may be inaccurate.

Implementation of this finite element scheme as a finite difference method places two key constraints on the model. First, a constant spatial discretization must be used. Second, separate solution algorithms are required based upon the type of flow regime anticipated (subcritical or supercritical). Therefore this scheme cannot model transitions between the two. This need for separate solution algorithms is associated with the different boundary conditions required for each flow regime. For example, in the case of subcritical flow, one boundary condition must be specified at each end of the domain and a double-sweep solution algorithm is employed. In the case of supercritical flow, two boundary conditions are specified at the upstream end of the domain and therefore the system of equations is solved sweeping from upstream to downstream. Only the subcritical algorithm has been implemented in the ONE-D model (Environment Canada 1988).

Fourier stability analysis of phase and amplitude accuracy

Description of the analysis method

A linear stability analysis allows us to examine the amplification and phase characteristics of a particular numerical scheme. The amplification characteristics are determined by examining the "algorithmic damping" of the numerical scheme, which is the ratio of the computed peak magnitude to the actual peak magnitude. This quantifies wave peak attenuation which occurs as a result of errors in the numerical calculations, rather than as a result of some physical influence (such as friction). In an analogous manner, phase accuracy refers to the ability of the numerical scheme to propagate these waves at the correct speed. This behavior is described by the "relative celerity," which is the ratio of the computed wave speed to the actual wave speed.

The analysis used here may be described as a Fourier (or von Neumann type) linear stability analysis. Roache (1982) provides a description of the theory and methodology. Details of the implementation are provided by Hicks (1996), and by Hicks and Steffler (1995). Because this is a linear analysis, it

does not predict instabilities associated with nonlinearities in the problem. Nevertheless, such an analysis is a valuable aid in the determination of the appropriate discretization of a problem for a particular numerical scheme and equation formulation. The applicability of the results to the nonlinear case is examined through wave propagation tests afterwards.

When the algorithmic damping is less than 1, the wave peak attenuates. When it is greater than 1, numerical amplification occurs. The latter case is an unstable situation which may lead to large oscillations and possibly even a breakdown in the solution. To quantify the algorithmic damping, we must consider frictionless flow; otherwise we would not be able to distinguish between physical attenuation and numerical dissipation effects. This is done by considering the equations in [19] which describe shallow water gravity waves (dynamic waves in horizontal, frictionless channels). These waves have two characteristic velocities: $V + c$ (for progressive waves) and $V - c$ (for regressive waves). When the relative celerity is less than 1, the numerical scheme is propagating these waves too slowly; and when it is greater than 1, the waves are propagated too quickly. Nonlinear waves are comprised of multiple wave components, each with their own frequency. Therefore, the relative celerities obtained from the linear stability analysis for different spatial resolutions give an indication of the behavior for wave components of the same resolution. When wave components are propagated at different speeds in the nonlinear case, the wave will spread out and the peak will be lowered. This is called wave diffusion.

An important parameter in examining the ability of numerical schemes to propagate waves accurately, both in terms of peak magnitude and wave speed, is the Courant number, C:

$$[23] \quad C = \frac{\alpha \Delta t}{\Delta x}$$

where α represents the speed of propagation of the modelled wave (e.g., $\alpha = V + c$ for progressive, dynamic waves).

For any given numerical scheme, numerical dissipation and diffusion effects, and therefore solution accuracy, will vary depending upon the Courant number used. This characteristic behavior is strongly dependent upon the number of nodes used to describe the wave, with accuracy improving as the number of nodes per wavelength (i.e., the grid resolution) increases. It is important to recognize that both stability and accuracy are important considerations in determining an appropriate Courant number and grid resolution for a particular application. Consequently, explicit and implicit models may require similar Courant numbers, but for different reasons. In the case of explicit schemes, stability is usually the dominant issue. In contrast, the dissipative nature of this fully implicit formulation means that the primary consideration in choosing an appropriate Courant number, when applying the ONE-D model, is accuracy.

Historical information

Despite the lack of sophisticated mathematical software at the time of their study, Gunaratnam and Perkins (1970) did manage to conduct a limited linear stability analysis on the finite difference scheme which has been implemented in the ONE-D model. However, they included the friction term in their stability analysis and, therefore, the physical attenuation due to friction masked the numerical damping behavior. They concluded that for 90% or better accuracy, at least 100 nodes per wavelength should be used and that the Courant number should not exceed 5.5. Morse (1991) reported that, provided 50 to 100 nodes were used to describe a wave profile, "many applications of ONE-D have shown that accurate results are still obtained as long as σ [the Courant number] $\leq$15."

Since 1970, research into the behavior of numerical techniques applied to the St. Venant equations has clearly established that the fully implicit approach leads to an excessive amount of artificial diffusion. Therefore, although stability may be guaranteed through the use of a fully implicit model, large time step increments can lead to very inaccurate results. This explains the need for an excessively large number of nodes to describe a wave profile. In fact, for most implicit numerical schemes, the use of 100 nodes to describe a wave profile would result in good phase and amplitude accuracy, regardless of the Courant number used. However, the use of such a high grid density is only practical for modelling long flat waves. When modelling surge propagation, this may be an unreasonable limitation and a far better approach may be to simply limit the Courant number. It is stressed that the latter is a more flexible approach than that recommended by Gunaratnam and Perkins (1970), as it facilitates the use of the scheme for a greater variety of flow scenarios.

An important consideration in the modelling of dynamic waves is the fact that there are two wave components: a progressive wave and a regressive wave. Examples of these are seen in the classic dam break problem. The progressive wave is the surge that propagates downstream, while the regressive wave is the deficit that propagates upstream into the depleting reservoir. In the case of waves propagating on still water (Fr = 0), there is no difference in the physical behavior of progressive and regressive waves. However, for waves propagating on a moving flow (Fr > 0), the regressive wave will propagate at a different speed and will display different phase and amplitude accuracy from the progressive wave for many schemes.

Progressive waves (all Froude numbers) and regressive waves (Fr = 0)

Figure 1 illustrates the amplitude and phase characteristics obtained for the ONE-D scheme from the linear stability analysis at a Froude number of zero (wave propagation in still water) and Courant numbers ranging from 0.1 to 5.0. In the figures, the spatial resolution is equal to the wavelength, L, divided by the spatial discretization, Δx. Therefore, the spatial resolution represents the number of nodes per wavelength. As the Courant number is based upon the progressive wave velocity in all cases, these results represent progressive wave behavior for all Froude numbers, not just for a Froude number of zero.

As Fig. 1*a* illustrates, the numerical scheme used in the ONE-D model is highly dissipative at high Courant numbers, and this numerical dissipation is nonselective (affecting all wave components rather than just the high frequency components associated with numerically generated instabilities). For example, the linear stability analysis suggests that if we were to use a Courant number of 5 and only 10 nodes to describe a wave, the peak amplitude would diminish to 20% of its original value in a single time step. In contrast, for the case where 100 nodes were used, the wave peak would only be lowered

Fig. 1. Amplitude and phase accuracy of the ONE-D scheme for progressive waves (all Froude numbers) and regressive wave (Fr = 0): (*a*) algorithmic damping; (*b*) relative celerity.

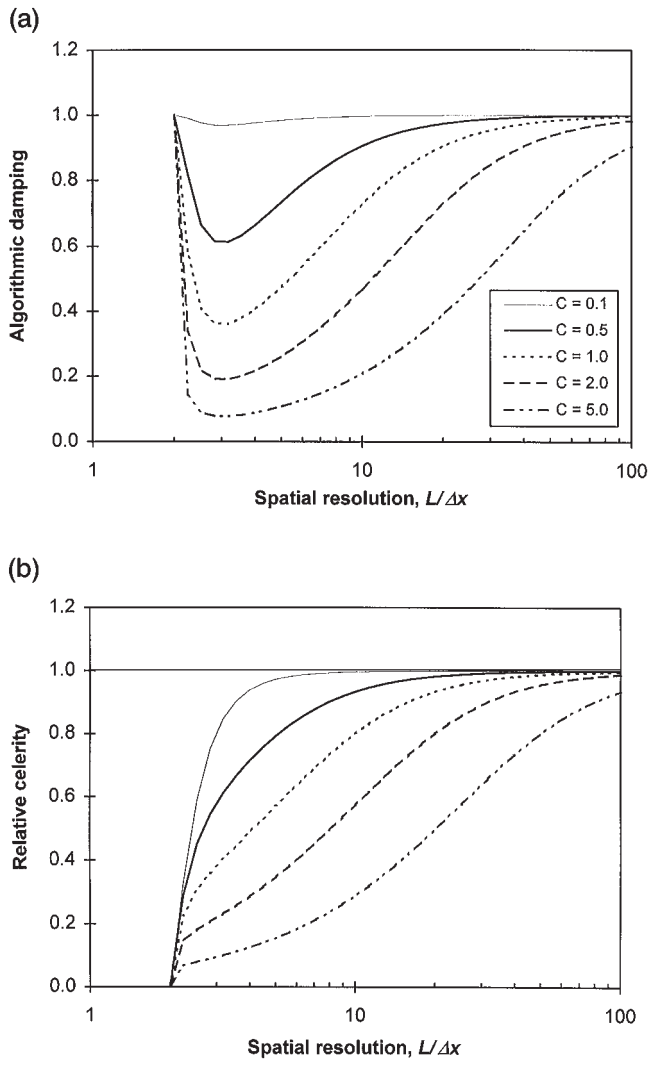

Fig. 2. Amplitude and phase accuracy of the ONE-D scheme for regressive waves (Fr = 0.5 and 2.0): (*a*) algorithmic damping; (*b*) relative celerity.

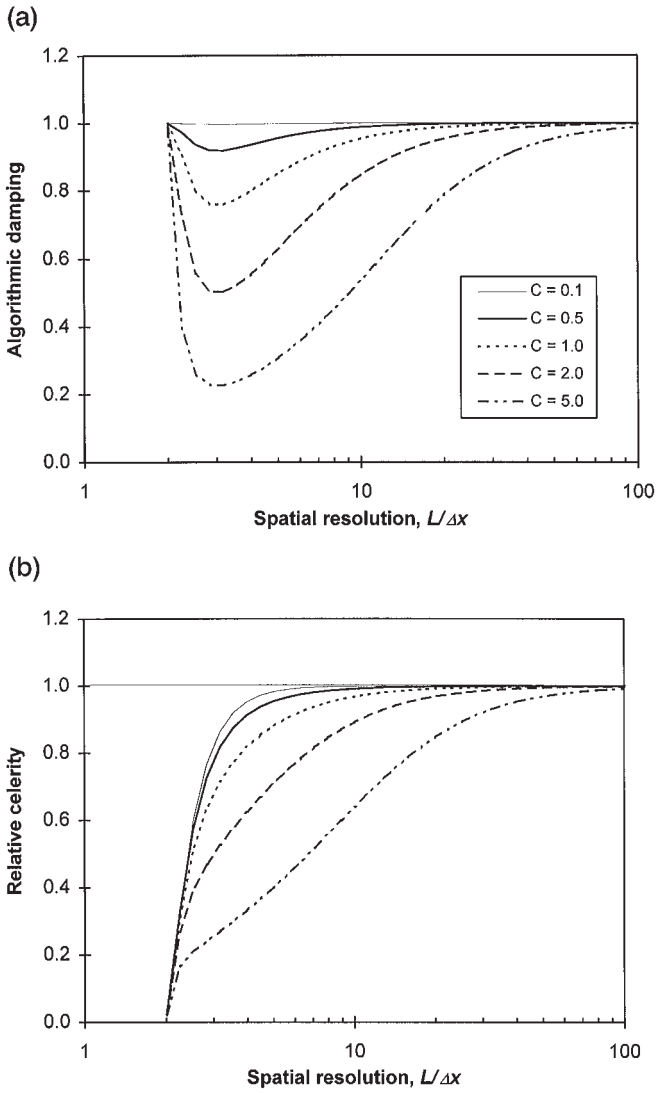

to 90% of its original value in one time step. This illustrates the reasoning behind Gunaratnam and Perkins' (1970) recommended discretizations. However, this combination of large time steps and small space steps is not necessarily optimum, as the same accuracy can be achieved with a more reasonable number of nodes per wavelength simply by decreasing the time step increment (effectively reducing the Courant number). For example, at a Courant number of 1, only about 20 nodes per wavelength are required to achieve the same accuracy as 100 nodes at a Courant number of 5. This behavior has important implications for modelling steep waves where it is not feasible to use 100 nodes to describe the wave front. Furthermore, the reduction in the time step increment does not necessarily lead to greater computational effort, as the number of arithmetic operations per time step is $53(2N - 1)$, where N is the number of nodes (Gunaratnam and Perkins 1970). Therefore, the reduction in the number of nodes compensates for the additional time steps required.

In the phase diagram of Fig. 1*b* it is seen that most wave components are propagated too slowly and that this phase error increases with decreasing wavelength (as Δx is held constant). This means that in a nonlinear problem, a separation of wave components would develop. This wave diffusion would attenuate the wave peak, further decreasing the amplitude accuracy. The figure also shows that increasing the spatial resolution, or decreasing the time step increment (i.e., the Courant number), would reduce phase error.

A feature of particular interest in Fig. 1 is the fact that for $2\Delta x$ waves, the type associated with numerical errors, the algorithmic damping and relative celerity are very close to 1.0 and 0.0, respectively. That is, these wave components are negligibly propagated and attenuated by this scheme and might therefore be expected to remain at the location where they were generated, accumulating over time.

Effect of Froude number on the regressive wave behavior

Figure 2 illustrates the regressive wave amplitude and phase characteristics for the numerical scheme in the ONE-D model at a Froude number of 0.5 and Courant numbers ranging from

Fig. 3. Comparison of the results of the wave propagation test at $t = 17.34$ s for varying Courant number.

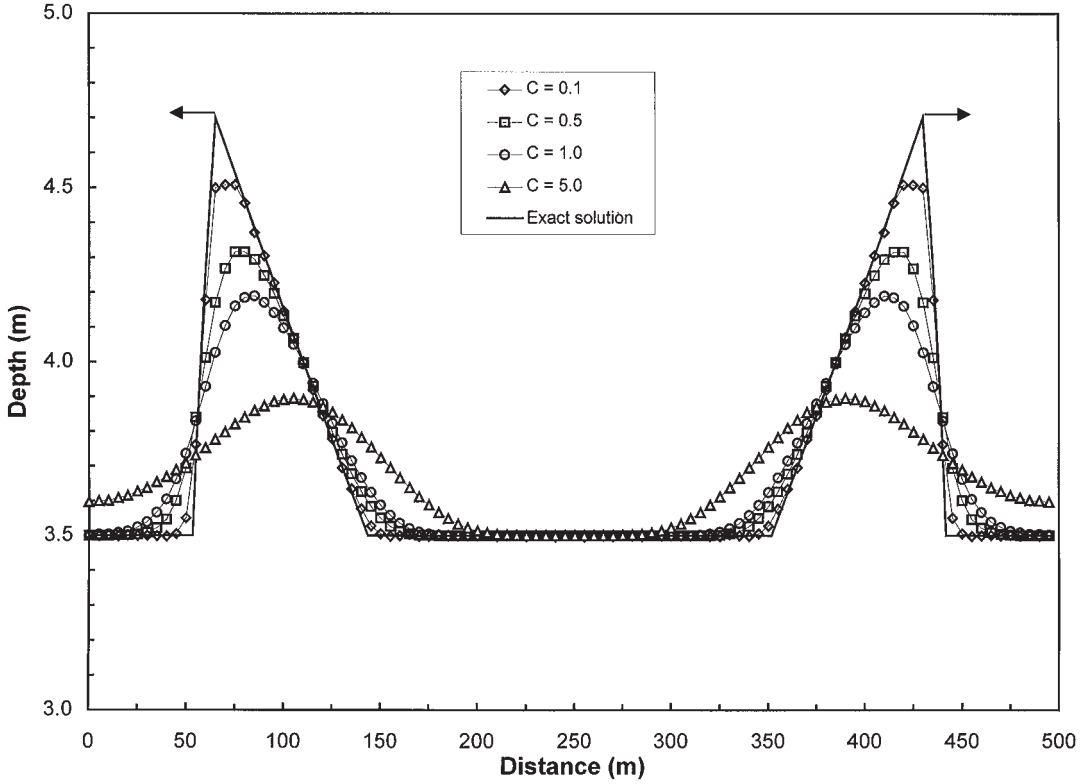

0.1 to 5.0. These results also describe the behavior for the reciprocal of this Froude number (i.e., for Fr = 2.0), as well. Comparing Figs. 1 and 2, we see that the scheme implemented in the ONE-D model is less dissipative for these regressive waves than for the progressive waves and phase accuracy is better as well, especially at the higher Courant numbers. Nevertheless, the damping is still large and unselective, and the phase error is significant, at large Courant numbers.

Discussion of results

These results identify a number of expectations about the performance of this scheme. For example, we would expect to see significant amplitude damping of any waves for spatial resolutions less than 100, when modelled at the recommended Courant number (>5). At lower Courant numbers we would expect that the algorithmic damping would be less, resulting in greater wave peak accuracy though possibly at the expense of persistent, numerically generated, high frequency disturbances. We might also expect to see high frequency wave components trailing the physical waves in this case, as these would not be expected to be damped at the lower Courant numbers.

Nonlinear wave propagation tests

To further examine the behavior of this numerical scheme, two test problems were conducted. The first test scenario involved the simple propagation of waves in still water. The intention was to validate the general tendencies predicted by the Fourier analysis, as well as to point out any effects of the nonlinearities which are missed in that linear stability analysis. The second test was a classic (subcritical) dam break problem. This surge propagation problem was useful for assessing model performance for dynamic flows with steep water surface gradients and, in particular, the conservation properties of Gunaratnam's six-point finite difference scheme. By eliminating the friction and slope terms from consideration, exact solutions based on the method of characteristics could be obtained easily, thus facilitating a quantitative assessment of performance. Because the ONE-D model has not been set up to handle these idealized cases (specifically frictionless flow), a computer program implementing the scheme was developed based on the equation formulation in [19].

It is important to remember that although it may seem idealistic to consider these simplified cases, the elimination of the friction and slopes terms from consideration allows for the determination of exact solutions based on the method of characteristics. This is the only way in which to make a quantitative assessment of the accuracy of the numerical solutions. Furthermore, this is the only way to facilitate an evaluation of the linear stability analysis, remembering in particular that the artificial damping associated with the numerical solution technique is indistinguishable from friction, in terms of its effect on attenuating the wave peak.

Propagation of progressive and regressive waves in still water

For this test, the geometry consisted of a unit-width section of a horizontal, frictionless, rectangular channel. A total of 100 nodes were used, with a uniform spatial discretization of 5 m. A zero discharge boundary condition was specified at each end of the domain throughout the simulation. The initial depth condition was taken as 3.5 m, except in the vicinity of the disturbances.

Fig. 4. Results of the spectral analysis of the wave propagation test for a Courant number of 5.

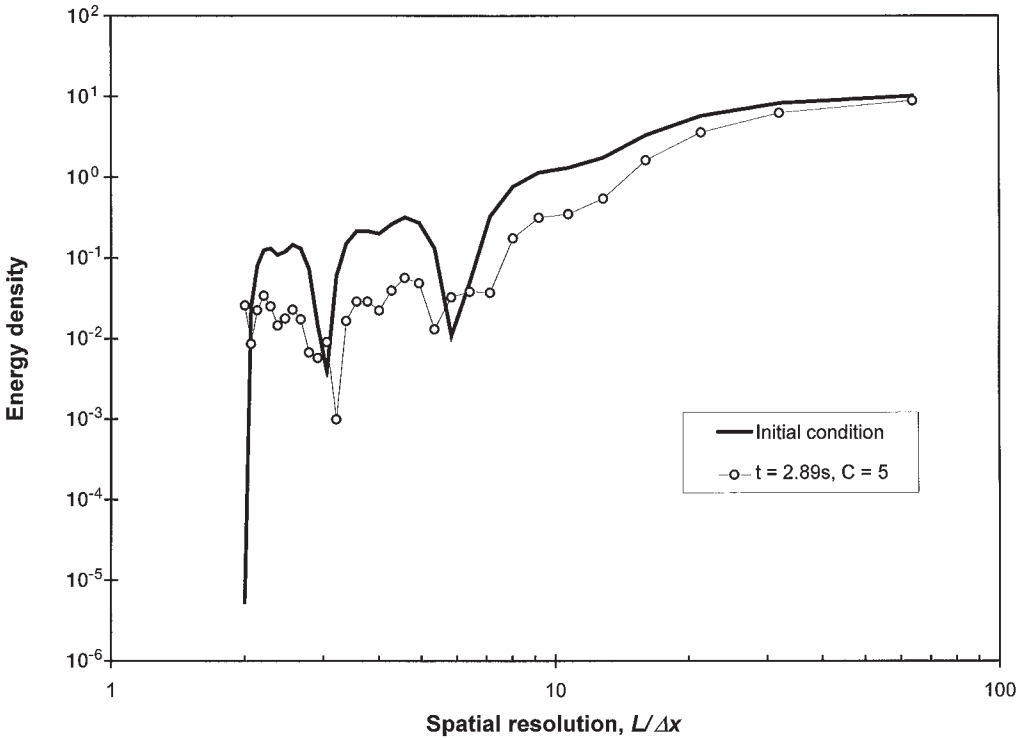

Table 1. Mass conservation and peak magnitude errors in the wave propagation problem.

	Error (%)	
Courant number	Mass conservation	Peak magnitude
0.1	–0.1	–3.4
0.5	–0.4	–8.2
1.0	–0.6	–10.8
5.0	–1.0	–17.1

To facilitate the computation of an exact solution, the initial condition was set as two identical disturbances, one progressive and one regressive, each initially prescribed over 20 nodes. The tests were run at time step increments of 0.0578, 0.289, 0.578, and 2.89 s, corresponding to Courant numbers of 0.1, 0.5, 1.0, and 5.0, respectively. Results were presented at $t = 17.34$ s, after the disturbances had each traveled exactly 150 m. The peaks, each of depth 4.70 m, were located at 65 and 430 m, respectively, by that time.

Figure 3 illustrates the results of the simulation and Table 1 presents the mass conservation and peak amplitude error for this range of Courant numbers at $t = 17.34$ s. Mass conservation is good (within 1%) but, as expected from the linear stability analysis, amplitude damping and wave diffusion (due to phase error) are evident. The results for $C = 5.0$ are particularly inaccurate, with the peaks propagated too slowly and the computed wave peak amplitudes 17.1% below the actual value. Both phase and amplitude accuracy increase with decreasing Courant number, with the results at $C = 0.1$ exhibiting primarily wave diffusion effects. It is a particular advantage of this numerical scheme that the method accuracy improves with decreasing Courant number. This is not a general rule. For example, for the four-point implicit finite difference scheme used in the NWS DAMBRK model (Fread 1988), solution accuracy is optimum at a Courant number of 1 and decreases for both lower and higher Courant numbers.

Although the test results confirm that the amplitude accuracy is poor at high Courant numbers, the damping effect is noticeably smaller than that predicted by the linear stability analysis. This result is associated with the nonlinearities in the problem, which can be examined through a spectral analysis. This analysis involves taking a Fourier transform of the flow depth profile both for the initial condition and after one time step. The results of this analysis for a Courant number of 5 are shown in Fig. 4, and are presented in terms of the energy densities associated with the various wave components. This energy density may be interpreted as the amount of energy contained within each of these wave components. In the figure, the smaller spatial resolutions represent the higher frequency (shorter wavelength) disturbances and we see that most of these shorter wave components are damped by almost an order of magnitude over one time step at this Courant number. The magnitude of this damping effect is consistent with what was predicted by the linear stability analysis. At the same time, the longer wave components are accurately modelled, with negligible energy density damping over one time step, again as predicted by the linear stability analysis.

Another apparent inconsistency between the predictions of the Fourier analysis and the results of this nonlinear test is that we do not see the persistence of numerically generated $2\Delta x$

waves in the solutions. Here, again, the spectral analysis is useful, as Fig. 4 illustrates evidence of the nonlinear transfer of energy between wavelengths, known as aliasing. For example, the initial condition exhibits a deficit of $2\Delta x$, $3\Delta x$, and $6\Delta x$ wave components, yet after one time step the energy densities at these wavelengths have increased. The increase is particularly significant for the $2\Delta x$ waves, indicating that there is no damping of $2\Delta x$ wave components, a result that is consistent with the linear stability analysis prediction. Therefore, even though these $2\Delta x$ disturbances do not appear in the solution, they would be expected to accumulate over time and consequently might be expected to present a problem in real world applications which involve significantly longer reaches and simulation periods.

Subcritical dam break test

This test simulates the wave propagation resulting from the instantaneous failure of a dam in a horizontal, frictionless channel. It is a rigorous test for Gunaratnam's six-point finite difference scheme, since it is not feasible to model the surge front profile with 50 to 100 nodes, as is currently recommended. Furthermore, from a computational perspective, the more dynamic the wave the greater the potential for numerical instabilities. Therefore, the simulation of an "instantaneous" failure represents the most difficult possible scenario in terms of the difficulty presented to the numerical scheme. If the optimum discretization relationship is determined under this scenario, then the scheme can be expected to provide a stable solution for the more practical case of a more prolonged dam breach (or ice jam release) event. The elimination of the friction and slope terms in this case are also not limiting to the practical applicability of the results, since it can be shown that the magnitude of these terms are negligible in the zone just downstream of the dam (Henderson 1966). These terms only become significant further downstream when, as a result of the influence of friction, the wave spreads out and diffuses. The latter scenario is not a challenge to the stability or accuracy of any of the formulations considered here, as the spatial resolution at that point becomes very high (as the wave becomes very long).

For this test, the channel geometry consisted of a unit-width section. A total of 81 nodes were used, with a uniform spatial discretization of 25 m. The dam itself was approximated between two nodes, over 25 m at the centre of the domain. The discharge was initially set to zero at all nodes, and through the upstream half of the domain the initial flow depth was set to 10 m. For the downstream half, a depth of 5 m was specified. One boundary condition at each end specified a discharge of zero throughout the duration of the simulation. The tests were run at time step increments of 0.25, 1.25, 2.5, and 15 s, corresponding to Courant numbers of 0.1, 0.5, 1.0, and 6.0, respectively. Results were presented at $t = 60$ s.

Table 2 presents the mass and momentum conservation errors for each Courant number at $t = 60$ s. Figure 5*a* illustrates the results for Courant numbers of 0.5 and higher. As expected from the linear stability analysis, we see that adequate results can be obtained for the progressive wave if the Courant number is limited to 0.5. Nevertheless, algorithmic damping and wave diffusion are evident in the solutions. The fact that the leading edge of the surge trails the exact solution suggests that mass is not being conserved, and this is confirmed by the data in Table 2. It is significant to note that momentum conservation errors occur even at the lower Courant numbers, reflecting the fact that the conservation properties are strongly dependent upon the equation formulation used. Hicks (1996) has illustrated that, for the six-point implicit finite difference scheme, the conservation characteristics of the symmetric formulation used in the ONE-D code are significantly inferior to the more conventional nonsymmetric formulations used in most models of this type.

Table 2. Conservation errors in the dam break problem.

	Conservation error (%)	
Courant number	Mass	Momentum
0.1	–0.4	–3.4
0.5	–0.8	–3.5
1.0	–1.1	–3.4
6.0	–2.7	–7.5

Figure 5*a* shows that the regressive wave is also quite diffused at the higher Courant numbers. As for the previous test, the fact that $2\Delta x$ oscillations are not seen trailing the propagating disturbances indicates that aliasing effects have not had time to accumulate over the short duration of this idealized test. However, these disturbances are seen in Fig. 5*b*, which presents the results for $C = 0.1$.

Discussion of results

The results of these nonlinear tests confirm the tendencies predicted by the linear stability analysis in that it has been shown that good phase and amplitude accuracy can be achieved at reasonable discretizations, provided that the Courant number is limited. Based on the results of the wave propagation tests, a maximum Courant number of 0.5 is recommended as suitable for most applications, assuming the use of at least 10 to 20 nodes to describe a wave profile. The computational effort required is comparable to that for the currently recommended use of 100 nodes with Courant numbers in excess of 5. It is not considered appropriate to develop separate criteria for long and short wave problems, as this would require a means of classification, which is an impractical requirement for real world applications.

It was found that errors in momentum conservation, and to a lesser extent mass conservation, occurred for the surge propagation problem and that these errors are not insignificant even at low Courant numbers. Based on similar findings for finite element methods (Hicks and Steffler 1995), these conservation errors are primarily attributed to the symmetric formulation used.

It was seen that wave aliasing could be expected to lead to the generation of high frequency disturbances and, as expected from the linear stability analysis, $2\Delta x$ waves would not be numerically attenuated. Although these did not present a problem for the short duration idealized test cases examined here, they can be expected to accumulate over time and might be expected to be a concern in practical applications.

For practical applications where friction is dominant, the issue of numerical wave diffusion and dissipation is less critical than for the dynamic situation represented by the dam break problem. Friction dominated problems tend to involve long flat waves, and in these cases the grid resolution required to define

Fig. 5. Comparison of the results of the dam break test at $t = 60$ s for varying Courant number: (*a*) $C = 0.5$, 1.0, and 6.0; (*b*) $C = 0.1$.

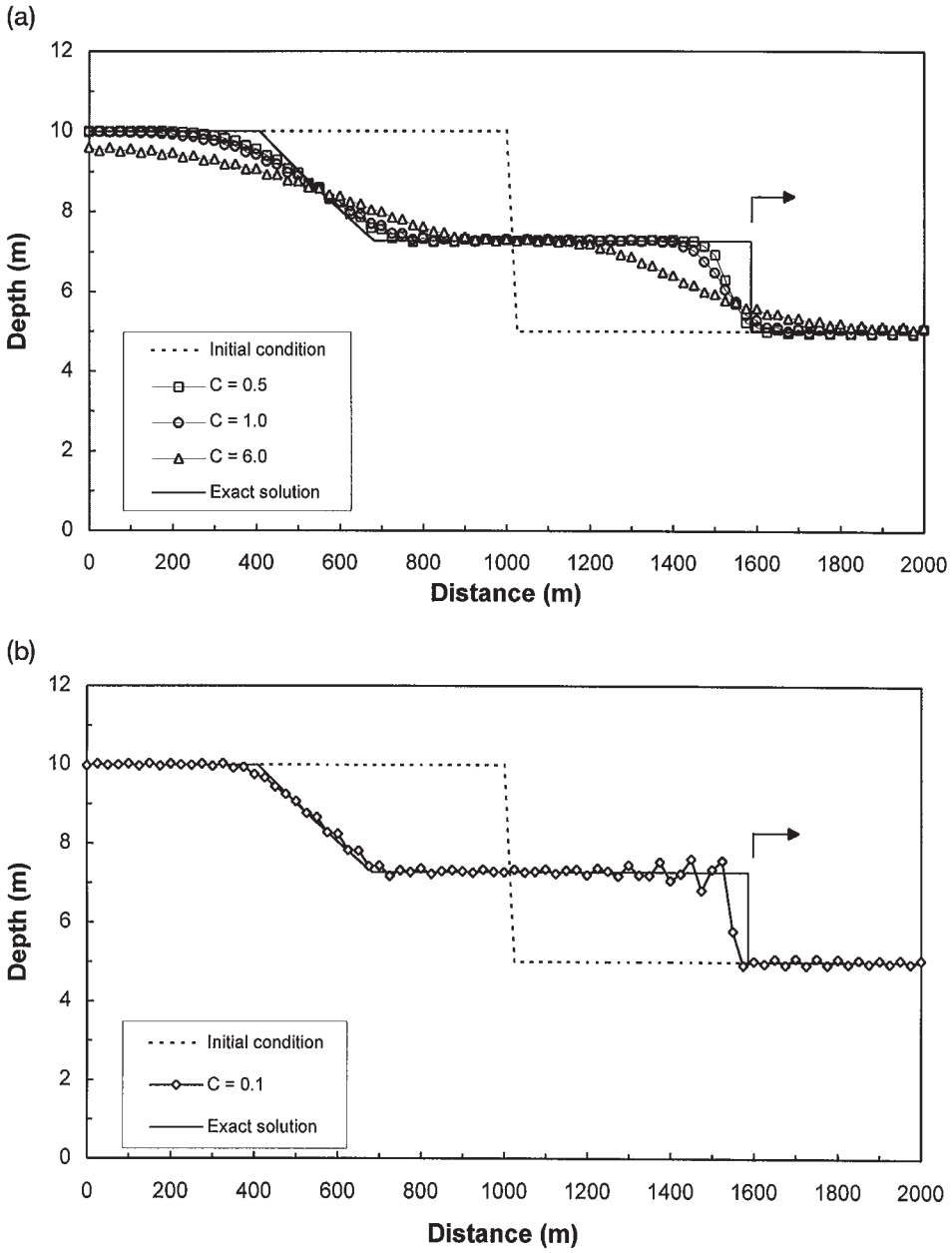

the channel geometry will likely be the limiting factor in determining model accuracy.

Summary and recommendations

This paper has provided a review of the details of the equation formulation and numerical scheme implemented in Environment Canada's ONE-D unsteady open channel flow model. In addition, the linear stability and accuracy characteristics of the implemented numerical scheme have been examined using a Fourier stability analysis and nonlinear wave propagation tests. The latter were also used to provide information on the mass and momentum conservation properties of the model.

The ONE-D model is based on a symmetric formulation of the St. Venant equations solved using Gunaratnam's six-point, implicit finite difference scheme, which is, in fact, a fully implicit finite difference implementation of the Bubnov–Galerkin finite element scheme. This finite difference implementation necessitates the use of an even grid spacing as well as separate solution algorithms for subcritical flow. Consequently, transitions between subcritical and supercritical flow cannot be modelled. In addition, only the subcritical flow algorithm has been implemented in the ONE-D model.

Based on the results of this investigation into the numerical behavior of the six-point, implicit finite difference method, a number of conclusions can be drawn about the expected performance of Environment Canada's ONE-D model.

1. This fully implicit formulation introduces nonselective artificial diffusion into the solution, particularly at high Courant numbers. This not only damps out numerical oscillations,

but physical wave components as well. In particular, it leads to a smearing of surge fronts. Thus the main issue in the application of the model becomes one of accuracy rather than stability.

2. The use of a symmetric formulation of the St. Venant equations contributes to mass and momentum conservation errors, particularly for shock propagation problems.

3. The conclusions of Gunaratnam and Perkins (1970), and Morse (1991), that accurate solutions could be obtained with this scheme for high Courant numbers (between 5.5 and 15) by using at least 50 to 100 nodes per wavelength does not represent an optimal implementation of this scheme.

Despite these apparent limitations, it has been shown that reasonable accuracy can be obtained with the implemented scheme and equation formulation, provided appropriate discretizations are used. However, it is concluded that the guidelines regarding the recommended relationship between the time and space step increments and the number of nodes used to describe a wave profile should be changed. It has been shown here that a better compromise between stability and accuracy can be obtained at much lower, and more reasonable, spatial discretizations (10 to 20 nodes to describe the wave profile) by limiting the Courant number to 0.5. The added computation expense of the additional time steps is more than offset by the reduced number of nodes required, particularly for shock propagation problems where it is not feasible to use 100 nodes to describe the wave profile. Improved mass conservation accuracy can be expected when the Courant number is limited, as well.

Acknowledgments

This project was funded in part through a research contract with Environment Canada (Contract No. KE501-5-5032). This support is gratefully acknowledged. The author would also like to thank Mr. Malcolm Conly, who initiated and supervised the contract; Mr. John Kerr who supplied source code and reference material; and Dr. Peter Steffler who provided valuable input and advice.

References

Dailey, J.E., and Harleman, D.R.F. 1972. Numerical model for the prediction of transient water quality in estuary networks. Hydrodynamics Laboratory, Massachusetts Institute of Technology, Cambridge, Mass., Report No. 158, RT72-72.

Environment Canada. 1988. Environment Canada One-Dimensional Hydrodynamic Model — computer manual. Water Modelling Section, Environment Canada,

Fread, D.L. 1988, The NWS DAMBRK Model: theoretical background/user documentation. Office of Hydrology, National Weather Service (NWS), Silver Spring, Md.

Gunaratnam, D.J., and Perkins, F.E. 1970. Numerical solutions for unsteady flows in open channels. Hydrodynamics Laboratory, Massachusetts Institute of Technology, Cambridge, Mass., Report No. 127.

Hicks, F.E. 1996. Fourier stability analysis of the numerical algorithm in the ONE-D model. Department of Civil Engineering, University of Alberta, Edmonton, Alta., Environment Canada Project KE501-5-5032 Report.

Hicks, F.E., and Steffler, P.M. 1990. Finite element modeling of open channel flow. Department of Civil Engineering, University of Alberta, Edmonton, Alta., Water Resources Engineering Report No. 90–6.

Hicks, F.E., and Steffler, P.M. 1995. Comparison of finite element methods for the St. Venant equations. International Journal for Numerical Methods in Fluids, **20**: 99–113.

Katapodes, N.D. 1984. A dissipative Galerkin scheme for open-channel flow. ASCE Journal of Hydraulic Engineering, **110**: 927–944.

Martinson, K., Sydor, M., Marcotte, N., and Beltaos, S. 1993. RIVICE model update. Proceedings of the Workshop on Environmental Aspects of River Ice (7th Workshop on the Hydraulics of Ice Covered Rivers), Saskatoon, Sask., NHRI Symposium Series No. 12, pp. 3–20.

Morse, B. 1991. Mathematical modelling of sediment transport and bed-transients in multi-channel river networks under conditions of unsteady flow. Ph.D. thesis, Department of Civil Engineering, University of Ottawa, Ottawa, Ont.

Roache, P.J. 1982. Computational fluid dynamics. Hermosa Publishers, Albuquerque, N. Mex.

Wood, E.F., Harley, B.M., and Perkins, F.E. 1972. Operational characteristics of a numerical solution for the simulation of open channel flow. Hydrodynamics Laboratory, Massachusetts Institute of Technology, Cambridge, Mass., Report No. 150, RT72-30.

List of symbols

A	cross-sectional area perpendicular to flow
B	total top width of a cross section
B_o	constant top width of a cross section
c	wave celerity
C	Courant number
Fr	Froude number
g	acceleration due to gravity
h	depth of flow in a rectangular channel
j, n	spatial and temporal indices
N	number of computational nodes
q_L	lateral inflow
Q	discharge
S_f	friction slope
V	cross-sectionally averaged longitudinal velocity
t	temporal coordinate
x	longitudinal coordinate
z	water surface elevation
Δt	time step increment
Δx	space step increment
α	speed of propagation of the modelled disturbance
λ_+, λ_-	characteristic velocities
ψ	source terms in the symmetric equations